

Spatial and Temporal Trends in Salinization in the Northeast Branch of the Anacostia River

GEOL394 - 4/25/2019

Julian Leal

Advised by Dr. Sujay Kaushal | Advised and assisted by Ricky Dubbin, Kelsey Wood, Joseph Gallela, and Jenna Reimer

ABSTRACT

Freshwater salinization is a growing environmental problem globally but with local impacts. However, the spatial extent of salinization in watersheds and its impacts are not always known in urban river networks across finer spatial scales. I hypothesized that there are increasing spatial gradients of salinity within stream networks (specifically the Northeast Anacostia system) that traverses through urbanized environments. This means that anthropogenic activity increases salinity in freshwater and salts accumulate in watersheds. Salinity, the concentration of all salts in the water, can be studied from major base cations in streams, calcium (Ca^{2+}), sodium (Na^+), potassium (K^+), and magnesium (Mg^{2+}), as well as organic carbon, inorganic carbon, and nitrogen concentrations, which can be used as secondary indicators for salinity sources through sewage inputs. In this research, the spatial distribution of salinity in a stream is evaluated as a function of season. The hypothesis of spatial connection to salinity along the length of the stream was studied within the context of its hydrologic flowpath into increasingly urbanized areas further downstream, i.e. increasing impervious surface cover and decreased forest cover. It is also shown that seasonally there will be a cyclical shifts in overall salinity as well as the in concentrations of individual salt ions. These increasing salt concentrations show that salts don't always dilute downstream, even with increasing flow. A syndrome of freshwater salinization propagates through stream systems downstream.

INTRODUCTION

Freshwater salinization is increasing on a continental scale (Kaushal et al., 2018). Salinization can have pronounced effects on urbanized streams and rivers due anthropogenic inputs of major ions (Kaushal et al. 2017). Because they are inherently more connected (pipes, ditches, etc.), chemical fluxes can travel more quickly, so much so that Kaushal (2012) proposed this warrants a 4-dimensional approach to the urban watershed continuum across spatial and temporal dimensions. Major base cations as well as dissolved inorganic carbon (DIC) can have elevated concentrations in freshwater systems, draining urbanized watersheds compared with forested watersheds (Baker, 2008; Barnes and Raymond, 2009; Kaushal, 2013). Inorganic carbon and calcium concentrations in streams across the eastern U.S. have shown increasing trends over time (Kaushal, 2013). Freshwater salinization can impact corrosion of pipes, complicate drinking water treatment and safety, increase water hardness and toxicity of metals, and harm aquatic life (Kaushal 2017, Kaushal et al. 2018). Anthropogenic processes are the primary cause of this rise in salinity. Use of road salts (primarily sodium chloride) and agricultural lime (bears high calcium), drainage of wastewater from mines and fracking brines, and dissolution of urban karst (calcium is a primary component in concrete) are all major salinity increasers (Kaushal, 2017). For example, Scott (1976) reported a 50-fold sodium concentration increase in urban streams after road salt application. Ruth (2003) reported a 30-fold increase in sodium in urban streams in Helsinki, Finland, when spring flooding washed out road salts. Demers and Sage (1990) observed chloride concentrations 31 times higher downstream as compared to upstream from a major road whose salted runoff affects Adirondack streams in New York. Road salts disrupt the proportional contributions of nitrate and ammonium nitrogen to the mineral portion causing it to leach into nearby waterways (Green et al., 2008). Green et al. (2009) also looked at this leaching regarding dissolved organic carbon (DOC) and found that initially salinity increases yield higher organic carbon, but on a longer time scale, downstream organic carbon will decrease and only vary seasonally due to most of it being flushed away already. Kaushal (2014) examined organic carbon and nitrogen as well, finding that they can show erratic patterns. He proposed that

the urbanized waterway can act as a reactor modifying and disposing of carbon and nitrogen as well, depending on in stream processes and the degree of urbanization. Significant amounts of nitrogen can be removed by assimilation and denitrification in urbanized areas as well. Urban karst dissolution as a result of construction (bridges, buildings, drainage infrastructure, and pavement on road and parking lots) can also influence base cations such as calcium and magnesium and inorganic carbon (Davies et al., 2010; Kaushal, 2014). Carbonates present within urban impervious surfaces such as concrete may be directly dissolved by acid rain and enter streams.

METHODOLOGY

The areas of interest are the Northeast branch of the Anacostia River and Indian Creek, one of its tributaries. Nineteen grab samples (250 ml each) were collected over a 9.5 km stretch from the Capital Beltway (upstream) to where the northeast branch converges with the northwest branch into the Anacostia River proper (downstream). The stretch varies from more wooded reaches in the north to more urbanized in the south. A baseflow synoptic sample set was collected in fall on October 20th, winter on February 20th, and spring on April 18th, to compare seasonality effects (unfortunately due to utility and instrument difficulties which extended outside the time constraints of this paper, this final synoptic set of cation data doesn't appear in this paper). The data was normalized for differences in discharge with the data reported from the USGS gauge at Riverdale, right at sample site six as shown below. This gauge records discharge, gauge height, pH, specific conductance, etc.

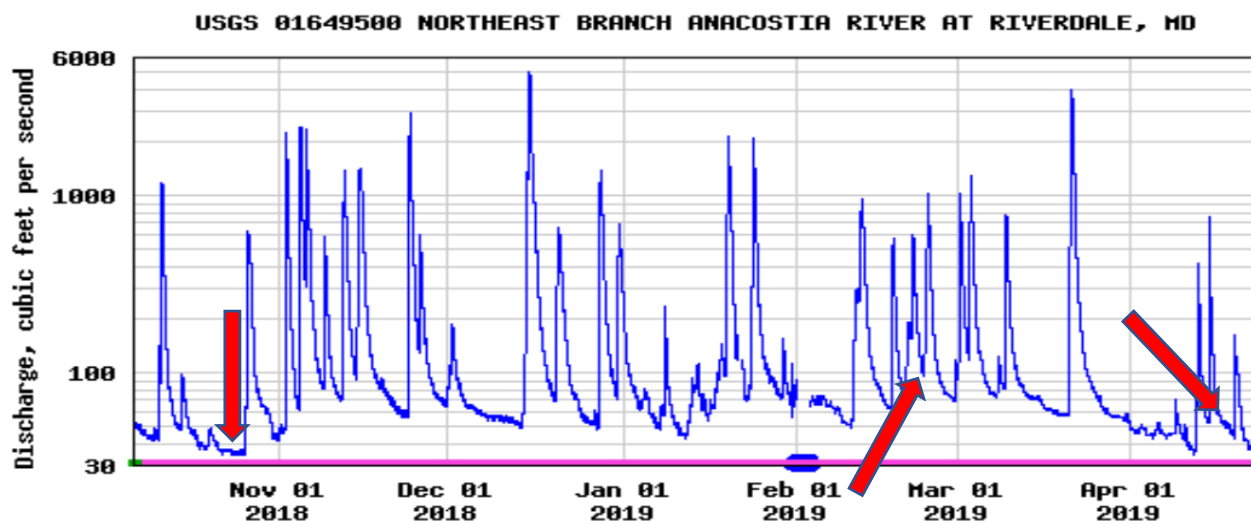


Figure 1. Discharge of the North East Anacostia over time (USGS, 2019). These data were used to normalize the cation data from the ICP-OES. Approximate sampling dates are denoted by the red arrows.

Each bottle (250 ml) was rinsed several times with the sample water before a final collection was made by completely submerging the bottle and capping it under water to avoid generation of headspace.

After collection, each sample was kept chilled until returned to the lab and was then frozen, to halt microbial activity, until ready to be analyzed. When that time came, each sample was set out and thawed at room temperature and filtered (pore size of 0.7 μm). Then, using a micropipette,

60 ml of the sample was acidified with 30 μ l of 15.8 molarity nitric acid to remove bacteria and other organics which could affect the ions of interest. This process also prevents adsorption by the bottle or precipitation of the ions.

Fifteen ml of each acidified sample was analyzed for major salt cations, sodium, calcium, magnesium, and potassium, via Inductively Coupled Plasma - Optical Emission Spectrometry (ICP-OES) on a Shimadzu ICPE-9820 Plasma Atomic Emission Spectrometer. In this process, the sample was completely ionized within the machine by an ultra-high purity argon plasma torch at a temperature of 7000 K. When the excited ions returned to their stable state, they released characteristic wavelengths. Thus, which ions are present was determined, as well as their concentrations based on the intensity of the light emitted (EPA, 2018; Shimadzu, 2006). Samples runs consisted of three blanks, 15 standards, the samples, and then another blank. The standards used were diluted with deionized water from a stock solution, IV-ICPMS-71A, which contained 10 μ g/ml of over 50 different cations, including the cations of interest. The standards were (in ppb) 2.5, 5, 10, 15, 50, 100, 250, 500, 1000, 5000, 10,000, 25,000, 50,000, 100,000, and 250,000. Each sample was analyzed in triplicate for each ion. After background corrections were applied, a quantitative average concentration was reported, with relative standard deviation, in mg/L. These values were then normalized to discharge and converted into fluxes (Table 1).

Another 25 ml of the initial filtered sample was analyzed using a Shimadzu Total Organic Carbon Laboratory (TOC-L) analyzer with a Total Nitrogen Measuring Unit (TNM-L). To produce the inorganic carbon (IC) data, the sample and acid are mixed and then sparged to isolate CO₂. Then the mix was cooled and run through a Non-Dispersive Infrared (NDIR) gas analyzer inside the Shimadzu. The NDIR analyzer drew the gas through a chamber and passes infrared light through it. Any infrared absorbed is attributed to the CO₂. The infrared intensity was compared to a control chamber with no CO₂ and the difference was converted into a measure of carbon in ppm (EPA, 2008).

The organic carbon (OC) analysis started the same way as the inorganic carbon, but once the sample was acidified and sparged, inorganic carbon was purged. Then purified air was added and the mix was combusted to produce CO₂, which was cooled and run through the NDIR gas analyzer.

Total Nitrogen (TN) analysis began by converting the nitrogen in the sample to nitrogen oxide (NO) through combustion. Then the NO was cooled in the carrier gas as it passed through a thermoelectric cooler. This cooled and dehumidified gas entered a chemiluminescence analyzer which converted the NO into an unexcited and excited phase of NO₂ by reacting it with ozone (O₃). When the excited NO₂ returned to ground state, its radiation was measured photoelectrically. This peak was used to determine the nitrogen concentration (Shimadzu, 2008).

DISCUSSION

All four major salt base cations, potassium, magnesium, calcium, and sodium (Figures 4, 5, 6, 7) increased downstream in both fall and winter. Thus, salts are accumulating as streams enter more urbanized environments. This can be attributed to increased impervious surface weathering. Calcium and magnesium especially, and to a lesser extent sodium, are components of concrete via the limestone in it.

Also, all four cations had noticeably increased slopes and concentrations in the winter season relative to fall. Increased weathering most likely led to the calcium and magnesium increases. The concentrations increase more rapidly as you become more urbanized downstream and as the cations accumulate. Another parameter closely related to the weathering of impervious surface is inorganic carbon. The bicarbonate ion HCO_3^{2-} is the primary source of inorganic carbon in streams and it is also an ion that comes from the weathering of limestone in concrete. Figures 9 and 10 show this relationship and thus inorganic carbon follows the same trends as calcium and magnesium.

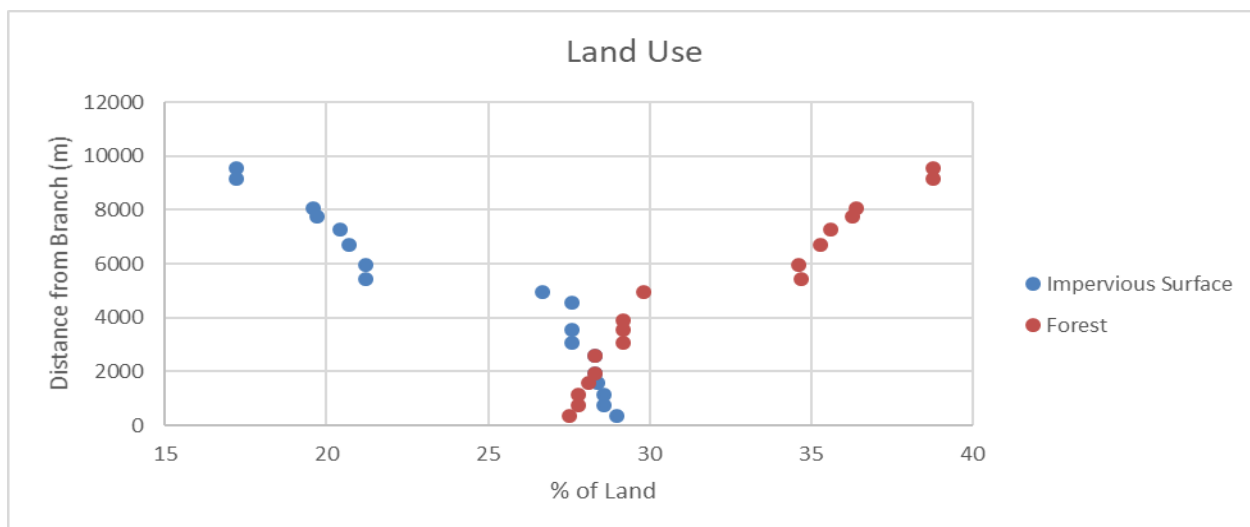


Figure 2. Land use data along the length of the stream. Each point was calculated from Streamstats (2019) by analyzing the drainage basin of each sample site and how much was covered by impervious surface and how much was forested. The discrepancy in percentage is unforested or developed land that isn't impervious. Impervious surface cover increases and forested area decreases from upstream to downstream. This serves as a proxy for urbanization and contributes to cations such as magnesium and calcium from weathering of these impervious surfaces (i.e. concrete).

Sodium is almost assuredly experiencing the steep increase in concentration as well as slope due to the use of deicing salts on the roadways which permeates streams via runoff. The closer you get to downstream, the more urbanized and road salt needed, as well as just overall accumulation. Sodium also has the effect of mobilizing the other major cations (Figure 11) as well as nitrogen and carbon (Figure 12), so it's large increase increases the other variables as well as seen.

Potassium, as well as nitrogen (Figure 13), can come from fertilizer and sewage, but is also under heavy biologic control. The fact that potassium sees these same increases downstream as the other cations, shows that it is being mobilized by this overall salinity rise. Despite biologic uptake, enough of a concentration of potassium is entering the water for it to accumulate downstream, especially in winter when biologic activity and therefore uptake is much lower.

The same trends are seen in organic carbon and nitrogen (Figures 14 and 15). Once again, these factors are heavily influenced by the presence of biota in the streams (like potassium, Figure 16), and nitrogen can be taken up by soil. The increases they see downstream, as well as in winter,

show their accumulation and mobilization, despite the lower levels of bioactivity. In spring, the beginning renewal of biologic activity brings their overall concentrations back down from uptake.

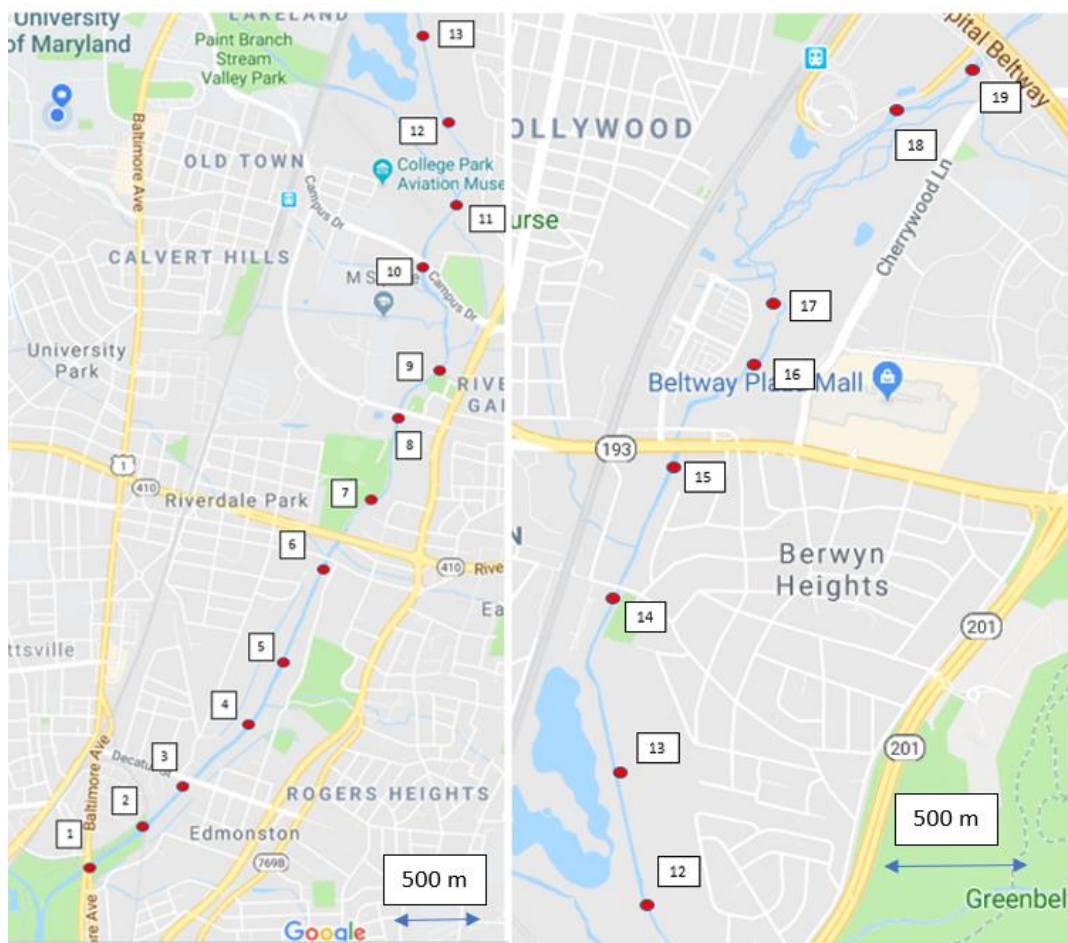


Figure 3. Sample locations – The right picture is Indian Creek, extending from the Capital Beltway past Lake Artemesia next to sample site 12. The left picture is the Northeast Branch of the Anacostia River from where Indian Creek feeds into it near sample site 11 until it merges with the Northwest branch into the Anacostia proper just south of sample site one. (Google Maps, 2018)

Figures 17 and 18 show the effect Paint Branch Creek, the creek that joins Indian Creek to form the Northeast Anacostia River has on the stream system's overall data set. In both Indian Creek and the Northeast Anacostia, the same overall trends of each variable are present. In the less urbanized Indian Creek, the slopes are less pronounced due to less accumulation and input from impervious surfaces or road salts. Then in the Northeast Anacostia, the values are higher due to the input of Paint Branch, but the trends are the same and are accelerated due to the quicker accumulation and larger source of impervious surface weather and road salt usage. I postulate that Paint Branch has a similar accumulation to Indian Creek and that addition leads to the jump at their convergence, but the same overall trending across the whole system. This means that this freshwater salinization syndrome can propagate along stream systems and watersheds in any sort of scale, continental or very localized. A salt map would be required to determine the scale of

each individual case, but I think it's reasonable to assume nearly every water system that has humans near it is experiencing a similar phenomenon and set of stressors.

This freshwater salinization syndrome has numerous potential effects on stream ecosystems. Aquatic life is highly sensitive to salinity levels in their ecosystems. Canedo-Arguelles et al. (2012) found that even short term salinity increases can cause significant declines in density, richness, and diversity of aquatic life as well as biotic quality indices. The increasing inorganic carbon that comes with impervious surface weathering can increase the pH of a stream to a level that is harmful to aquatic life (Finlay, 2003). Naidoo (1987) showed increased salinity and increased nitrogen (which can be mobilized from salinity as shown above) decrease stomatal conductance and tissue water potentials, thus affecting the plants' ability for nutrient uptake. In addition to effects on life, increasing salinity can have effects on agriculture and infrastructure as well (Pitman, 2002).

The process to remediate this continental scale change to freshwater ecosystems will be long and complex, but measures can be taken. Reducing or regulating road salts is an almost immediate thing that can help. Other deicers are available and being able to precisely control how much salt is used in each area can reduce excess salty runoff. Limiting or reducing impervious surface cover is another way to prevent this erosion into freshwater. Some locales offer grants to remove impervious surface cover or when building, utilize materials and designs that aren't impervious and won't erode negatively. For waters affecting drinking supplies, filters and water treatment plants can be put in place, though that only stops the effect at the human level, not at the source. Also, being able to properly contain wastewater, brines, etc. and keeping infrastructure that might shed salts away from areas that are close to the water table to prevent easy entry into the water system can hedge against increasing salinity.

SUMMARY

Anthropogenic processes such as the use of road salts and urban karst erosion are increasing salinity levels in freshwater on the continental scale. This research examined the spatial effects of this along the northeast branch of the Anacostia River and Indian Creek using synoptic baseflow sampling events to capture a temporal aspect of fluxes as well. The hypotheses of cyclical temporal fluxes and also increasing spatial gradients downstream were both supported. Increases in all major cations as well as other proxies were noted as they accumulated downstream in correlation to impervious surface cover. These trends were even more pronounced in the winter, likely due to road salting's effect. This also shows that this stream system isn't regulating itself over time but is steadily increasing in salinity. These processes are exacerbating the salt levels of freshwater in the Northeast Anacostia River showing that even small localized watersheds experience freshwater salinization syndrome.

BIBLIOGRAPHY

A. Baker, S. Cumberland, N. Hudson, Dissolved and total organic and inorganic carbon in some British rivers, *Area*, 40 (1) (2008), pp. 117-127

R.T. Barnes, P.A. Raymond, The contribution of agricultural and urban activities to inorganic carbon fluxes within temperate watersheds, *Chem. Geol.*, 266 (3–4) (2009), pp. 318-327

P.J. Davies, I.A. Wright, O.J. Jonasson, S.J. Findlay, Impact of concrete and PVC pipes on urban water chemistry, *Urban Water J.*, 7 (4) (2010), pp. 233-241

C.L. Demers, R.W. Sage Jr., Effects of road deicing salt on chloride levels in four Adirondack streams, *Water, Air, and Soil Pollution*, 49 (1990), pp. 369-373

Google Maps, Oct 18, 2018, Northeast branch of Anacostia Civer and Indian Creek.
www.google.com/maps

S. Green, R. Machin, M.S. Cresser, Does road salting induce of ameliorate DOC mobilization from roadside soils to surface waters in the long term?, *Environmental Monitoring Assessment*, 153 (2009), pp. 435-438, DOI 10.1007/s10661-008-0369-4

S. Green, R. Machin, M.S. Cresser, Effect of long-term changes in soil chemistry induced by road salt applications on N-transformations in roadside soils, *Environmental Pollution*, 152 (1) (2008), pp. 20-31

S.S. Kaushal, K.T. Bolt, The urban watershed continuum; evolving spatial and temporal dimensions, *Urban Ecosyst.*, 15 (2012), pp. 409-435

S.S. Kaushal, G.E. Likens, R.M. Utz, M.L.Pace, M. Grese, M., Yepsen, Increased river alkalization in the eastern US, *Environ. Sci. Technol.*, 47 (18) (2013), pp. 10302-10311

S.S. Kaushal, Delaney-Newcomb, K., Findlay, S.E.G., Newcomer, T.A., Duan, S., Pennino, J., Longitudinal patterns in carbon and nitrogen fluxes and stream metabolism along an urban watershed continuum, *Biogeochemistry*, 18 (1-3) (2014), DOI 10.1007/210533-014-9979-9

S.S. Kaushal et al., Human-Accelerated Weathering Increases Salinization, Major Ions, and Alkalinization in Fresh Water across Land Use, *Applied Geochemistry*, 83 2017, pp. 121–135. doi:10.1016/j.apgeochem.2017.02.006.

S. S. Kaushal, G. E. Likens, M. L. Pace, R. M. Utz, S. Haq, J. Gorman, and M. Grese, Freshwater salinization syndrome on a continental scale, *Proc Natl Acad Sci USA* January 23, 2018 115 (4) E574-E583; <https://doi.org/10.1073/pnas.1711234115>

O. Ruth, The effects of de-icing in Helsinki urban streams, Southern Finland, *Water Science and Technology*, 48 (9)(2003), pp. 33-43

W.S. Scott, The effect of road deicing salts on sodium concentration in an urban water-course, *Environmental Pollution*, 10 (2) (1976), pp. 141-153

EPA, Monitoring, 2008

https://archive.epa.gov/region6/6pd/rcra_c/pd-o/web/pdf/a4b-monitoring.pdf

EPA, Inductively Coupled Plasma—Optical Emission Spectrometry, 2018

<https://www.epa.gov/sites/production/files/2015-12/documents/6010d.pdf>

Shimadzu, Introducing a New ASTM Method for the Determination of Total Nitrogen, and TKN by Calculation, in Water Samples, 2017

https://www.ssi.shimadzu.com/sites/ssi.shimadzu.com/files/Products/literature/toc/Shimadzu_NewTestMethodTotalNitrogenWater_ASTMD8083-16.pdf

Shimadzu, Quality Assurance in Water Analysis – Determination of Selected Elements Using ICP-OES, 2006

https://www.ssi.shimadzu.com/sites/ssi.shimadzu.com/files/Products/literature/AAS/ICP_Water_analysis_News_03_2006_en.pdf

StreamStats: Streamflow Statistics and Spatial Analysis Tools for Water-Resources Applications, February 23, 2018, www.usgs.gov/mission-areas/water-resources/science/streamstats-streamflow-statistics-and-spatial-analysis-tools?qt-science_center_objects=0#qt-science_center_objects

USGS Current Conditions for USGS 01649500 Northeast Branch Anacostia River at Riverdale, MD, April 23, 2018, waterdata.usgs.gov/md/nwis/uv?site_no=01649500.

M. Canedo-Arguelles et al., 2012, Response of stream invertebrates to short-term salinization: A mesocosm approach, *Environmental Pollution*, v. 166, p. 144-151

G. Naidoo, 1987, Effects of Salinity and Nitrogen on Growth and Water Relations in the Mangrove, *Avicennia Marina* (Forsk.) Vierh., *New Phytologist*, v. 107, p. 317-325

J. C. Finlay, 2003, Controls of streamwater dissolved inorganic carbon dynamics in a forested watershed, *Biogeochemistry*, v. 62, p. 231-252

Pitman, M.G., and Läubli, A., 2002, Global Impact of Salinity and Agricultural Ecosystems: Salinity: Environment - Plants - Molecules, p. 3–20, doi: 10.1007/0-306-48155-3_1.

APPENDIX

Sample Site	Distance from Branch (m)	Mg normalized flux (mg/s)	K normalized flux (mg/s)	Ca normalized flux (mg/s)	Na normalized flux (mg/s)	IC normalized flux (mg/s)	OC normalized flux (mg/s)	TN normalized flux (mg/s)		
1	349	8693.173235	4969.11565	31793.44687	39352.72795	27958.22339	4049.77367	1268.402898		
2	765	7513.196947	3641.43268	27968.83535	30491.51462	24239.6573	3486.781474	1080.693862		
3	1,120	8368.343216	4217.03159	30012.12096	35488.78537	26003.20261	4693.501398	1182.959512		
4	1,590	6444.56466	3146.33628	24953.70154	24736.71283	21395.08671	2989.019468	1001.402892		
5	1,940	7984.442399	4008.38404	28554.34866	32756.68676	25117.05159	3773.484113	1194.972553		
6	2,570	6262.543488	2894.5433	25286.9024	22273.99488	21423.92454	3052.720941	928.943950		
7	3,060	7910.618743	4017.11108	27810.76902	30900.85447	24195.36905	3375.403336	1173.202441		
8	3,540	7117.526496	3579.33413	26022.17057	26742.15157	22926.25225	3101.061038	1082.028594		
9	3,900	7415.373925	3666.60456	26703.56261	29168.50685	23273.18188	3378.00067	1119.495509		
10	4,540	7135.247735	3491.51456	24640.38885	25972.30176	20530.48615	3131.898073	1172.083361		
11	4,960	6513.490485	3207.60368	22962.51104	23141.20762	19710.23321	3153.101224	1101.66444		
12	5,440	2375.892787	1480.62884	9426.096384	7575.310336	9370.142387	2027.686761	555.6662298		
13	5,970	2338.134971	1299.43881	9361.088823	6582.683464	9540.616554	1973.522698	521.4853134		
14	6,710	2255.940479	1297.47968	8580.107573	6529.252592	8534.067971	1948.312232	540.3375062		
15	7,270	2381.013246	1349.93099	8944.328019	7287.970978	9035.427656	1894.044276	554.0514301		
16	7,770	2549.810276	1411.13902	9272.037369	7970.698791	9776.306068	1880.840914	600.6490875		
17	8,050	2599.82751	1473.50472	9527.318203	8235.478447	10019.83211	2045.547514	620.8904829		
18	9,160	2254.485972	1319.96517	8145.23964	6581.644531	8796.131558	1897.040857	561.8033591		
19	9,530	1665.855862	927.085002	5540.781455	3342.576002	6493.216437	1601.756626	445.0732293		
	standard error	609.6337793	296.484501	2191.136471	2770.754593	1735.801	203.366	68.586		
Mg normalized		K normalized	Ca normalized	Na normalized	IC normalized	OC normalized	TN normalized	IC normalized	OC normalized	TN normalized
flux (mg/s)		flux (mg/s)	flux (mg/s)	flux (mg/s)	flux (mg/s)	flux (mg/s)	flux (mg/s)	flux (mg/s)	flux (mg/s)	flux (mg/s)
18433.44829		11038.31859	54647.83342	213969.3776	24107.57905	9542.979866	2816.674399	15766.66121	5477.371376	1547.020351
17650.84111		9925.244999	53113.47324	209234.8946	24214.9153	8583.995674	2948.066014	15139.96872	4890.81201	1505.828664
17493.0129		10715.47498	53041.60115	210291.1965	23603.51251	8510.766002	2812.812182	15234.45866	5020.923322	1361.856504
17300.55542		10719.97606	52538.49653	208296.5645	23767.03603	8530.872038	3064.745631	15443.92987	4999.462498	1404.189498
17024.10198		9724.293544	51388.54312	206081.2344	23098.4913	8317.038055	2830.322836	15368.86383	5181.546332	1431.192008
17026.9696		9105.6128	51844.096	205534.208	23437.74208	8426.63936	2739.57888	15408.74957	4882.108518	1369.615749
16626.40975		8741.460886	49627.31396	200272.663	22019.91631	11643.52513	2798.778975	14691.44834	4721.57288	1301.628717
16250.27916		8728.865121	49052.70025	194953.0394	21517.78451	9772.807203	2724.311506	14444.86308	4664.433844	1356.508404
14694.57514		7384.965967	49233.10645	187638.421	22298.07581	8738.876395	2472.205274	14248.46291	4810.677354	1339.034996
14844.78054		7538.728678	43743.24047	174972.9619	19386.6319	7012.879085	2487.31511	12597.82058	4368.414056	1207.622897
13133.06327		6752.273796	40644.75489	136138.0769	18244.25046	7071.31327	2504.24135	12414.35038	6255.337038	1172.107323
5737.0624		3263.2832	19053.3632	61370.7776	8925.605888	3708.563456	1332.682752	6164.720927	2994.441298	524.8591012
5728.858818		3157.144823	18921.9607	61470.23695	8904.821061	3715.394934	1242.995098	6175.563448	2904.060985	532.8204595
5486.67166		3122.079956	18015.93679	60189.60702	8236.149287	X	257.7507321	6082.528297	2978.331206	533.6535441
5590.341703		3078.738909	18431.92373	61574.77817	7680.643383	4272.762979	1284.158203	5997.261865	2891.138384	504.2751529
4823.778692		2824.645667	16609.7122	57487.50689	7098.414129	3776.47169	1067.198874	5866.709484	2860.669846	513.69762
4798.441966		2942.254539	16291.00668	57364.09017	6910.348832	3751.868204	1141.357801	5724.245066	2799.416967	512.5249434
4526.671095		2623.512717	14584.95206	47401.09418	6236.845656	2973.907297	1093.871404	4914.63082	2644.038369	451.1010058
4499.337922		2595.090573	14525.42164	47207.62033	6260.988144	2952.026239	1096.492194	4565.543731	2679.47973	488.9177211
1339.490999		761.2806983	3899.365527	16596.60631	1804.415	654.353	188.855	1060.657	268.334	101.471

Table 1. Complete data set. Cells highlighted orange are from the fall, blue from the winter, green from the spring, and yellow are standard errors for their respective column.

Figure 4.

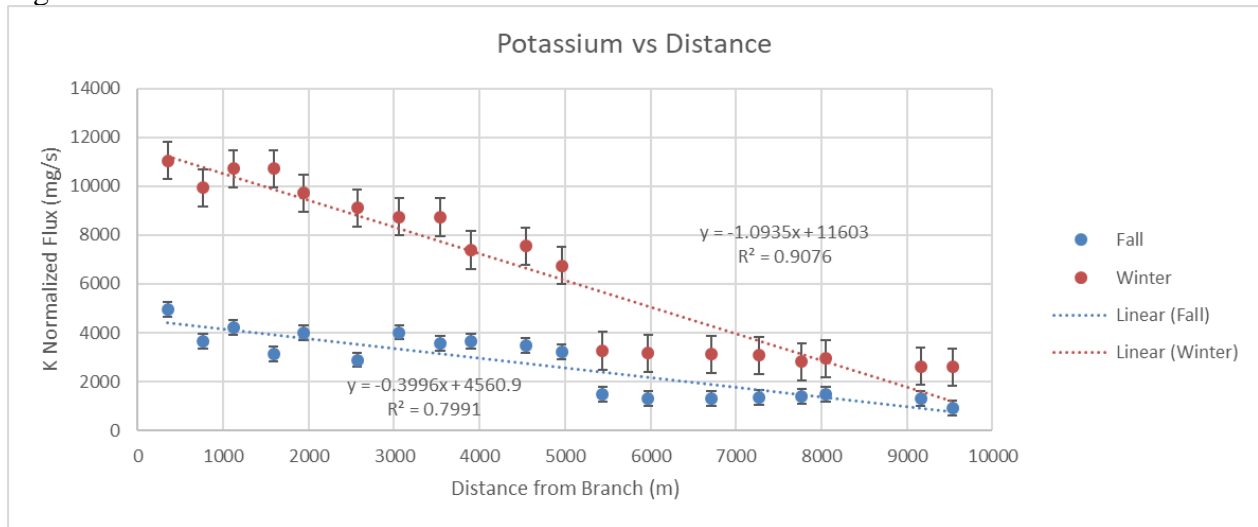


Figure 5.

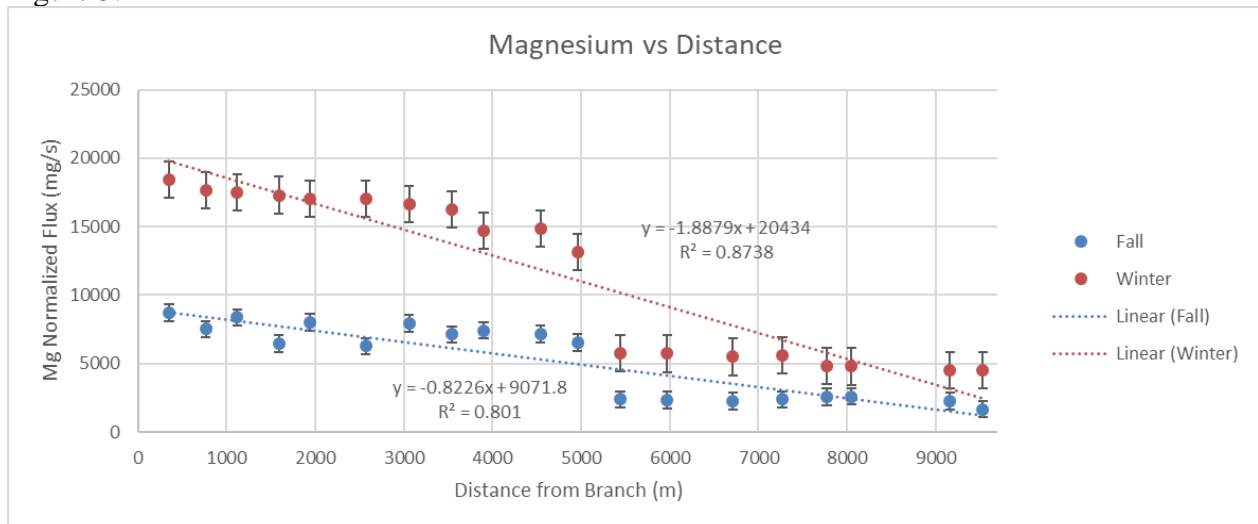


Figure 6.

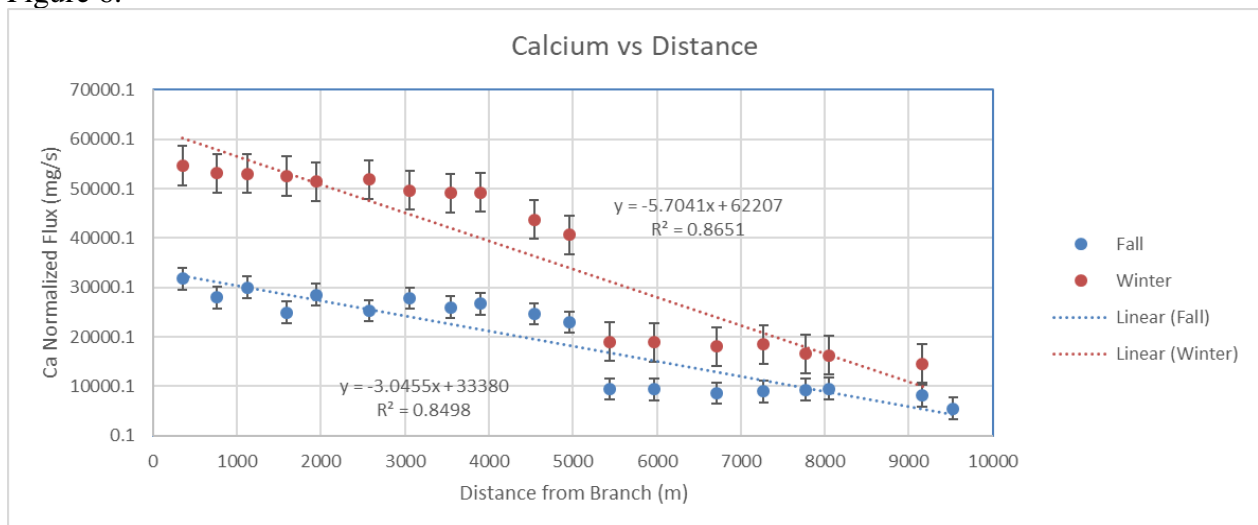


Figure 7.

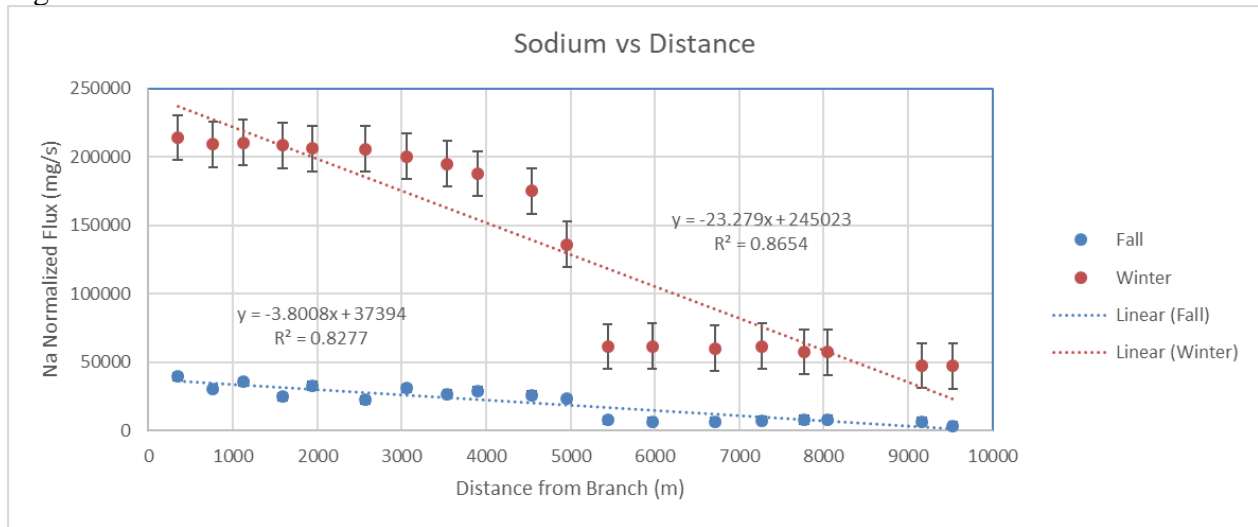


Figure 8.

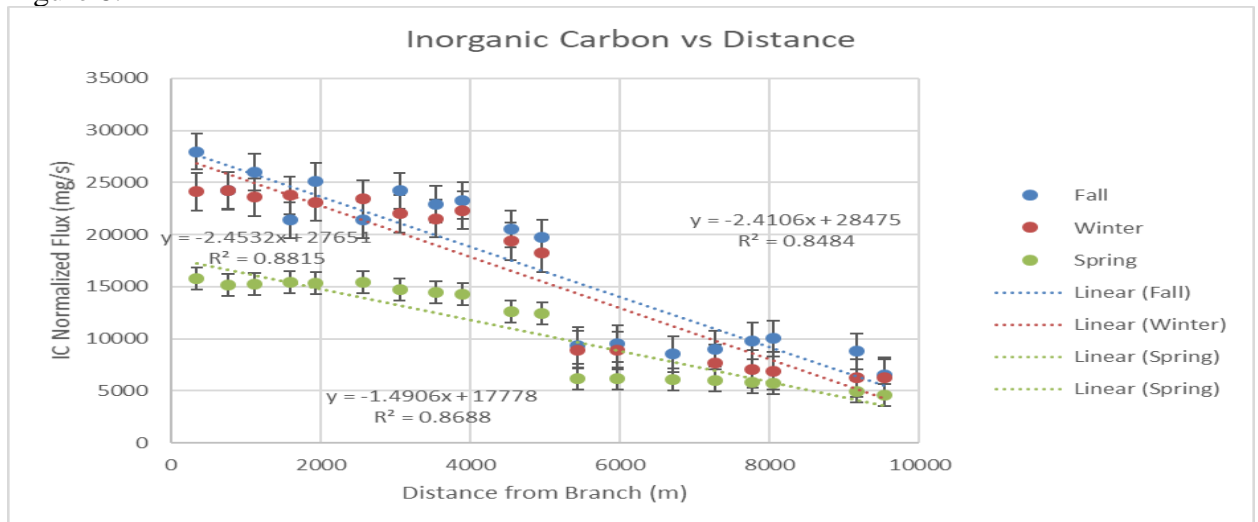


Figure 9.

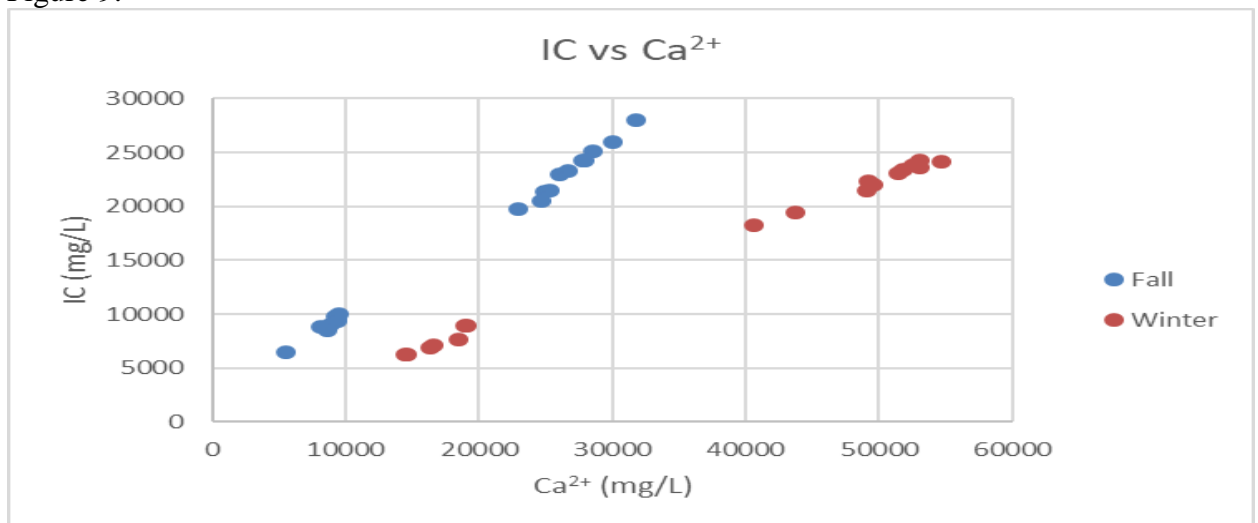


Figure 10.

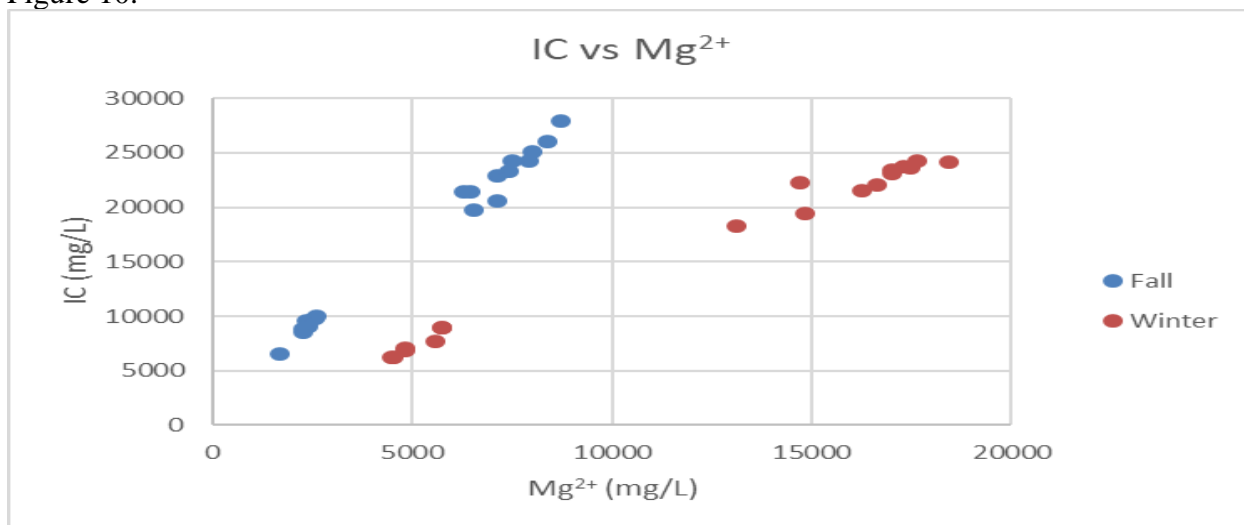


Figure 11.

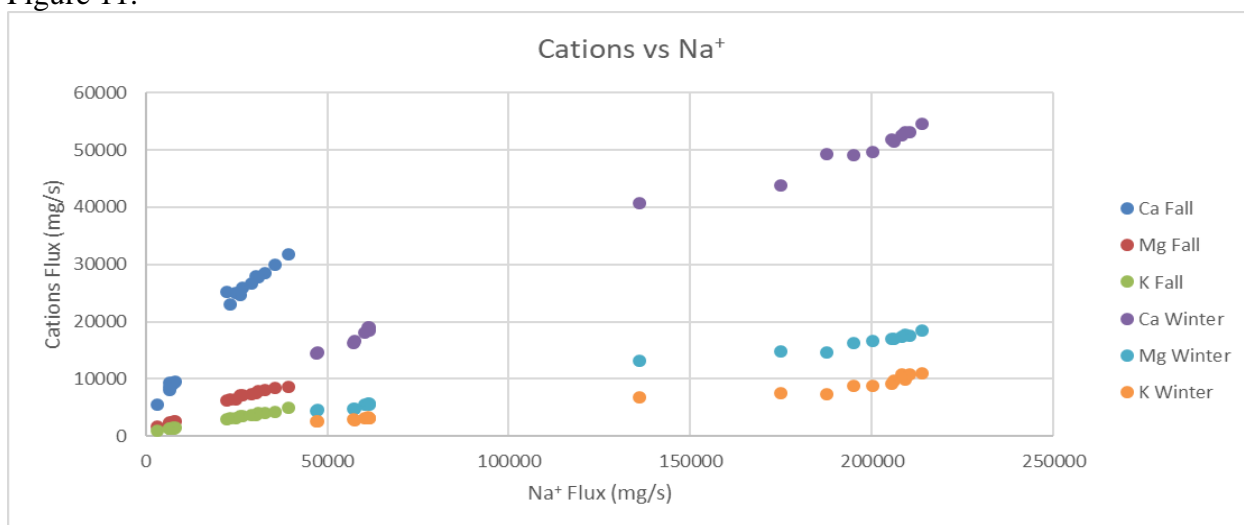


Figure 12.

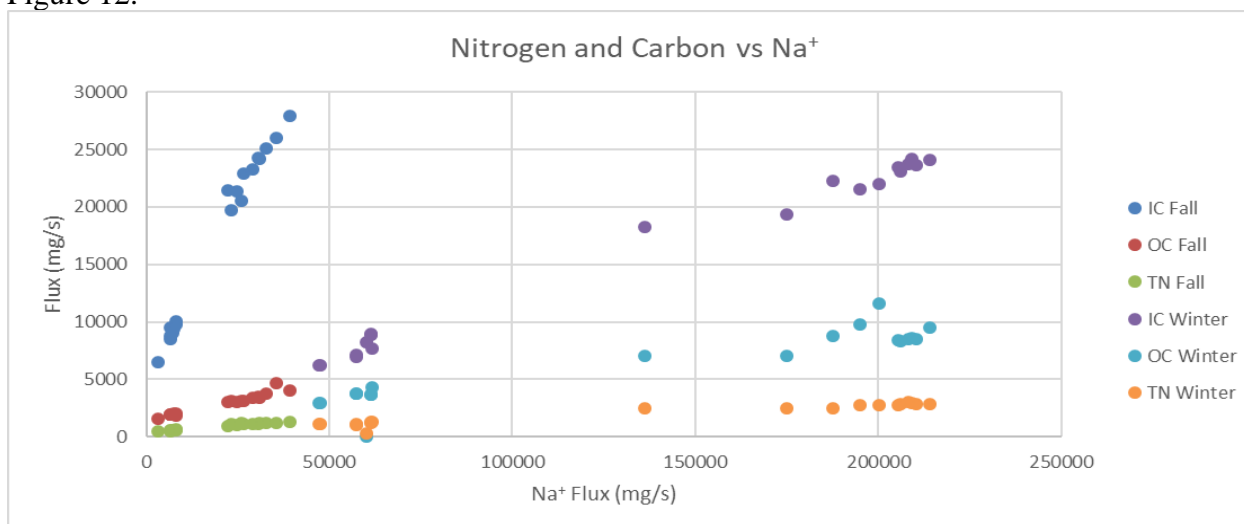


Figure 13.

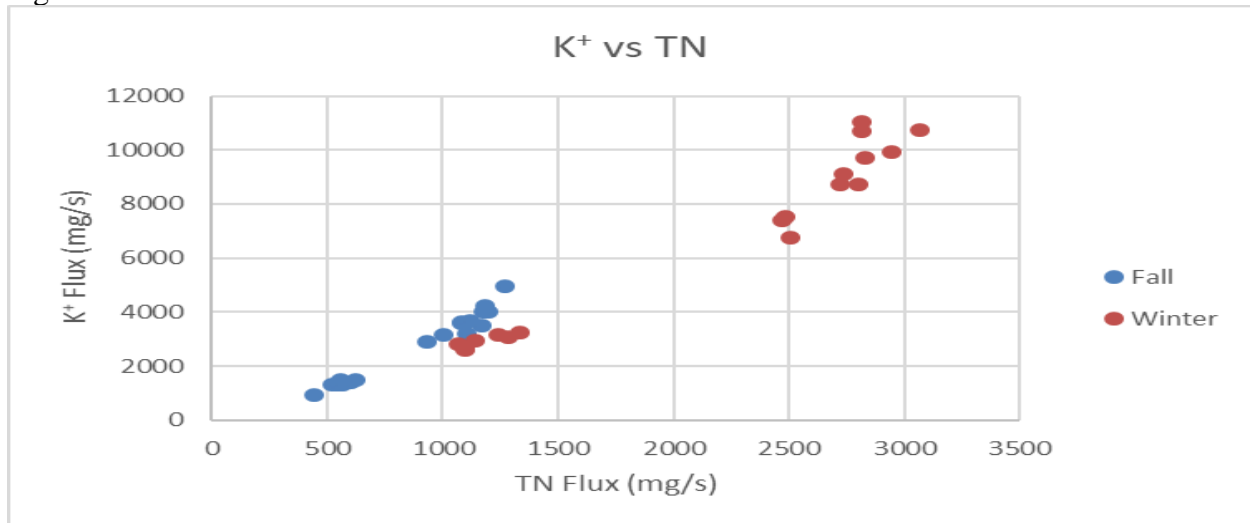


Figure 14

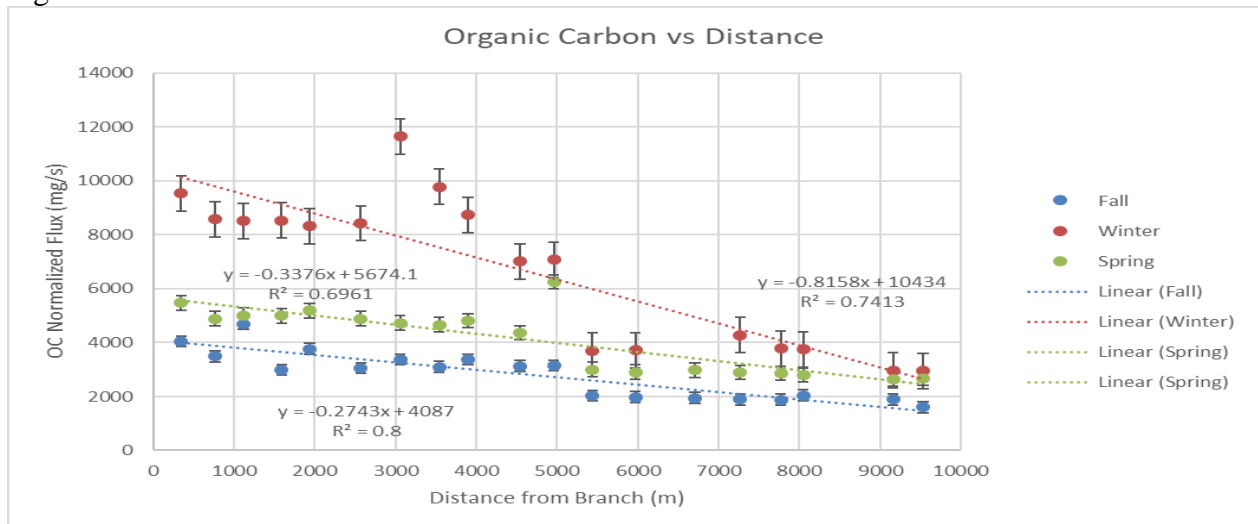


Figure 15

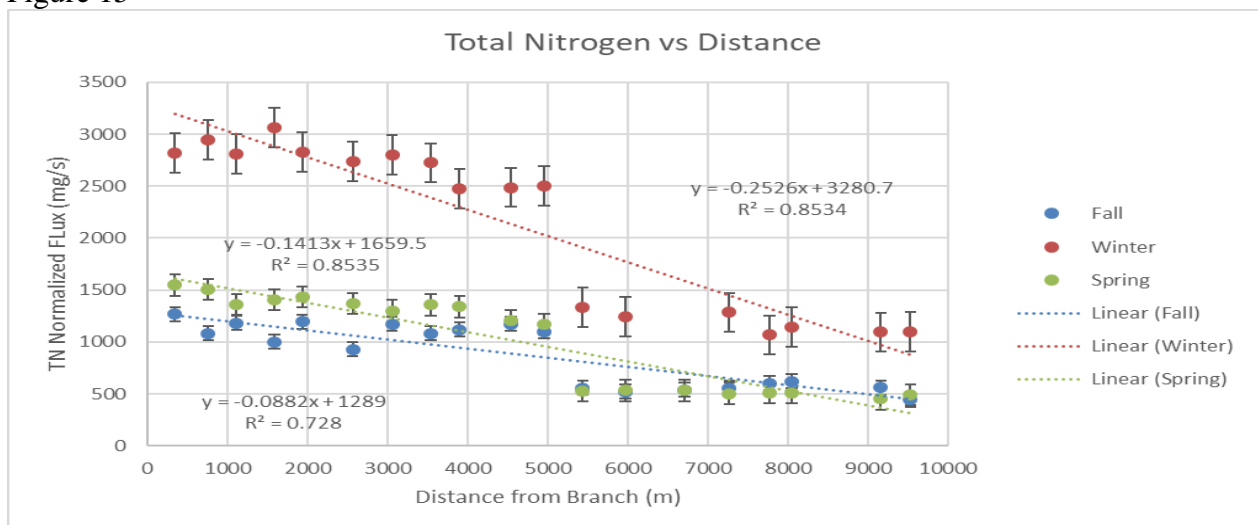


Figure 16

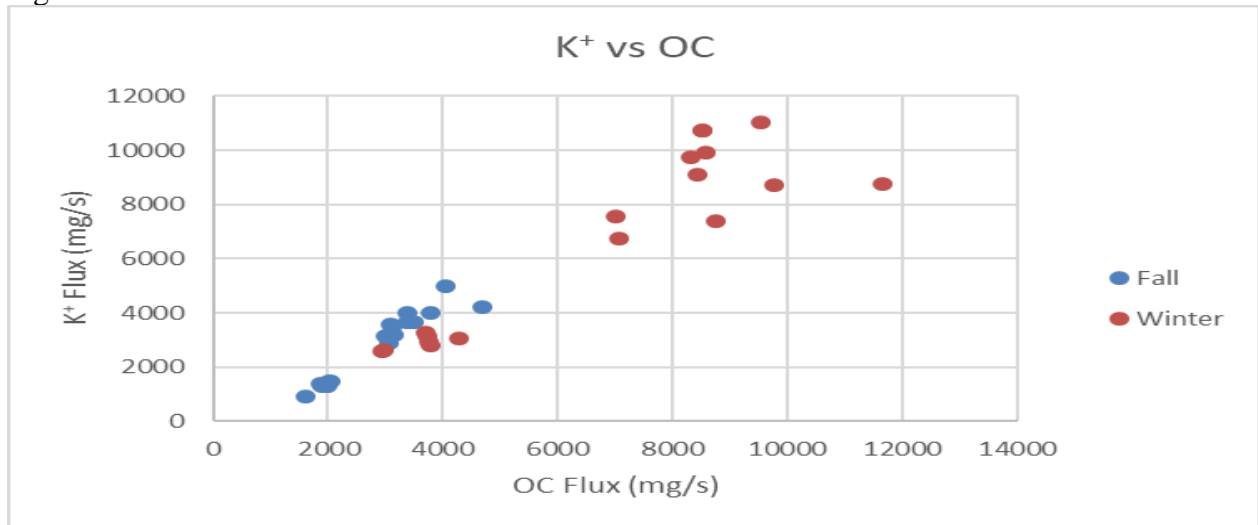


Figure 16

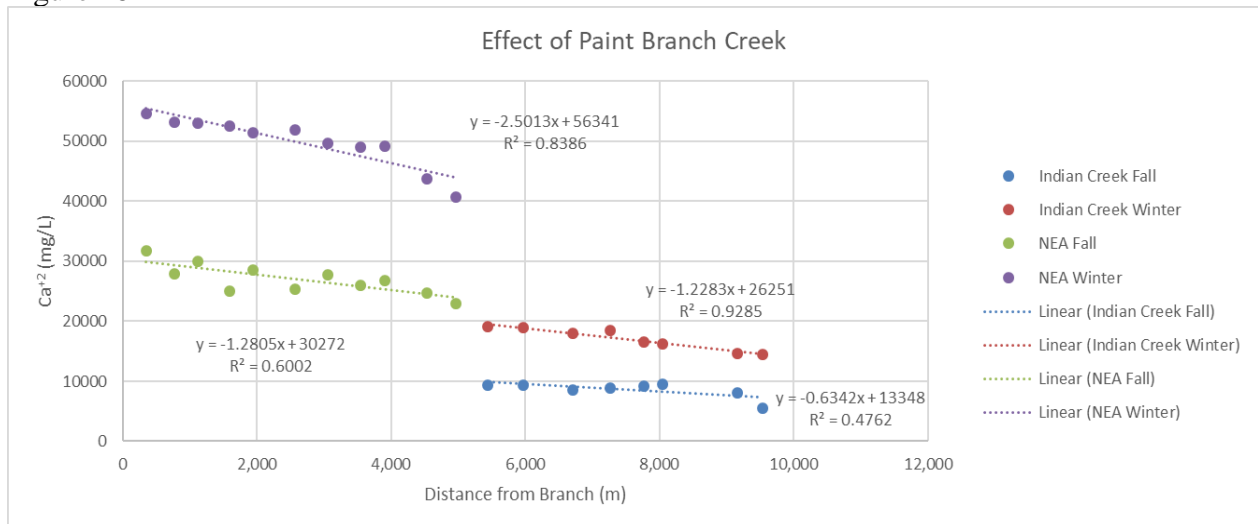
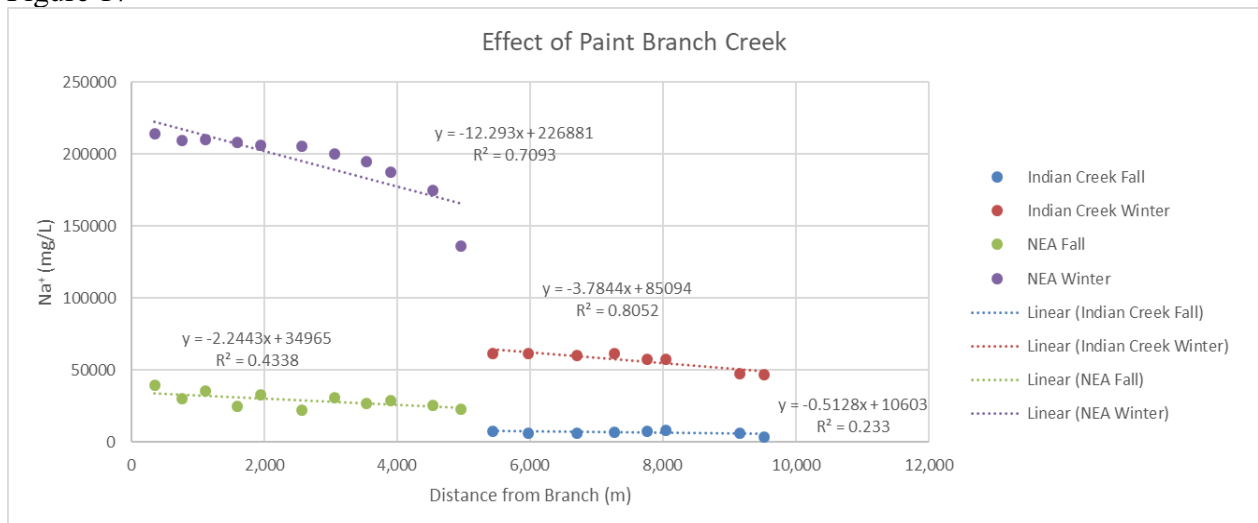


Figure 17



I pledge on my honor that I have not given or received any unauthorized assistance on this assignment/examination.

Julian Leal

4/25/2019